Nutrition 90 (2021) 111263

Contents lists available at ScienceDirect

Nutrition

journal homepage: www.nutritionjrnl.com

Basic nutritional investigation

Curcumin improves insulin sensitivity and increases energy expenditure in high-fat-diet–induced obese mice associated with activation of FNDC5/irisin

Tiande Zou Ph.D. [a], Shuo Li M.A. [a], Bo Wang Ph.D. [b], Zirui Wang Ph.D. [a], Yue Liu M.A. [a], Jinming You Ph.D. [a,*]

[a] Jiangxi Province Key Laboratory of Animal Nutrition, Jiangxi Agricultural University, Jiangxi, China
[b] State Key Laboratory of Animal Nutrition, College of Animal Science and Technology, China Agricultural University, Beijing, China

ARTICLE INFO

Article History:
Received 10 October 2020
Received in revised form 21 March 2021
Accepted 29 March 2021

Keyword:
Curcumin
Energy metabolism
Thermogenesis
High-fat diet
Irisin

ABSTRACT

Objective: Curcumin (Cur) has a beneficial role in preventing metabolic dysfunctions; however, the underlying mechanism are not yet fully understood. The aim of this study was to evaluate whether the beneficial metabolic effects of curcumin are associated with the regulation of energy metabolism and activation of fibronectin type 3 domain-containing protein 5 (FNDC5)/irisin.
Methods: We used cellular and molecular techniques to investigate the effects of Cur on C57 BL/6 mice that were fed either a control diet or a high-fat diet (HFD) with or without 0.2% Cur for 10 wk. Factors involved in energy metabolism, inflammatory responses, and insulin signaling, as well as the involvement of FNDC5/irisin pathway, were assessed.
Results: Cur alleviated adiposity and suppressed inflammatory response in white adipose tissue (WAT) of HFD mice. Meanwhile, Cur administration increased plasma irisin concentration and improved insulin sensitivity of HFD mice. Cur increased the oxygen consumption and heat production and reduced respiratory exchange ratio (RES) in HFD mice, which were accompanied by the enhancement of metabolic activity in brown fat and inguinal WAT. Additionally, the improvement of basal metabolic rate by Cur may be partly regulated by the FNDC5/ p38 mitogen-activated protein kinase (p38 MAPK)/extracellular signal-related kinase (ERK) 1/2 pathway.
Conclusions: These findings demonstrated that dietary Cur alleviated diet-induced adiposity by improving insulin sensitivity and whole body energy metabolism via the FNDC5/p38 MAPK/ERK pathways.

Introduction

Excessive energy intake and poor energy expenditure induce adipocyte hypertrophy and obesity, leading to inflammation, insulin resistance (IR), and metabolic disorders [1]. Adipose tissue is a key peripheral metabolic tissue responsible for energy homeostasis. Currently, two populations of uncoupling protein 1 (UCP1)-expressing thermogenic adipocytes, including classical brown adipocyte from brown adipose tissue (BAT) and brite/beige (brown in white) adipocytes from white adipose tissue (WAT), burn fatty acids and glucose for heat production, preventing ectopic lipid accumulation and IR [2]. Thus, pharmacologic and nutritional enhancements of thermogenic function in BAT and WAT have been considered effective therapeutic strategies against obesity and its associated diseases [3].

As a nutraceutical dietary supplement, curcumin (Cur) is a natural flavonoid component of turmeric (Curcuma longa) and has advantages in preventing adiposity and IR in diet-induced obesity in mammals [4,5]. Moreover, Cur has been recognized as having the potential to exert health benefits, such as anti-cancerous [6], anti-inflammatory [7], and hepatoprotective [8] properties. Even more importantly, Cur is characterized as safe and is tolerable even at high doses (12 g/d) in humans [9]. Dietary Cur was previously shown to promote thermogenic program in WAT and suppress diet-induced body fat accumulation [5,10]. Nevertheless, whether Cur supplementation can influence the whole body energy metabolism in obese mice and if so, what the molecular mechanisms involved are, remain unclear.

Irisin is a novel myokine and adipokine secreted into the circulation, produced by the cleavage of fibronectin type 3 domain-

This work was supported by the China Postdoctoral Science Foundation (2019M662270), the Jiangxi Province Postdoctoral Science Foundation (2019KY05), and Postgraduate Innovation Funding Project of Jiangxi Province (YC2019-S178). The authors have no conflicts of interest to declare.
*Corresponding author: Tel.: +86 791 8382 8479; fax: +86 791 8381 3503
E-mail address: youjinm@jxau.edu.cn (J. You).

https://doi.org/10.1016/j.nut.2021.111263
0899-9007/

Table 1
Ingredient and nutrition composition of the diets*

	LFD (MD12031)	HFD (MD12032)	HFD + Cur
Ingredient, %			
Casein	18.96	23.31	23.31
Cornstarch	29.86	8.48	8.48
Maltodextrin	3.32	11.65	11.46
Sucrose	33.17	20.14	20.14
Cellulose	4.74	5.83	5.83
Soybean oil	2.37	2.91	2.91
Lard	1.90	20.68	20.68
Mineral Mix	4.24	5.23	5.23
Vitamin Mix	0.95	1.16	1.16
L-Cysteine	0.28	0.35	0.35
Choline bitratrate	0.19	0.23	0.23
Red-Dye	0	0.01	0
Curcumin	0	0	0.20
Total calories (kcal/g)	3.85	4.73	4.73
Composition			
Protein (% energy)	20.00	20.00	20.00
Carbodydrate (% energy)	70.00	35.00	35.00
Fat (% energy)	10.00	45.00	45.00

Cur, curcumin; HFD, high-fat diet; LFD, low-fat diet
*Diets were purchased from Medicience Diets Co., Ltd. (Yangzhou, Jiangsu, China) and information of diet composition was provided by the company.

containing protein 5 (FNDC5). The FNDC5 expression is dependent on peroxisomal proliferator-activated receptor γ coactivator-1α (PGC-1α) [11]. The major role of irisin is known to promote browning of WAT and increases thermogenesis through upregulation of UCP1 expression [11–13], which counteracts the deleterious effect caused by excessive adiposity and thus leads to improvement in metabolic health. The circulating levels of irisin could be regulated by diet and pharmacologic agents [14]. However, it is unclear whether FNDC5/irisin participates in Cur-mediated energy metabolism. Thus, the aim of the present study was to investigate the effects of Cur supplementation on energy metabolism and insulin sensitivity in high-fat diet (HFD)-induced obese mice and to explore the role of FNDC5/irisin in mediating the beneficial effects of dietary Cur.

Materials and methods

Animals, diets, and experimental design

All animal experimental procedures used in this study were performed in accordance with the guidelines of the National Institute of Health and approved by the Animal Care and Use Committee of Jiangxi Agricultural University. Six-wk-old C57BL/6N male mice purchased from Vital River Laboratory Animal Technology Co. Ltd. (Beijing, China) were kept in a room with temperature-controlled conditions (23 ± 2°C, 12-h light/dark cycle) with free access to food and water. After 1 wk of adjustment period, mice were housed individually and randomly divided into three groups (n = 10/group) as follows: fed with the low-fat diet (LFD; 10% energy from fat, MD12031, Medicience Ltd.), a HFD (45% energy from fat, MD12032, Medicience Ltd.), or a HFD supplemented with Cur (HFD + Cur) for 10 wk. Detailed information on the diets is shown in Table 1. To prepare the Cur diet, Cur (Sigma-Aldrich, St. Louis, MO, USA) was mixed with powdered HFD diet at a concentration of 0.2% (dry feed, w/w), and pellets were then reconstituted. Previous studies suggested that dietary supplementation of 0.1% to 0.4% Cur effectively attenuated HFD-induced adiposity [4,8,15]. Thus, we chose an average, 0.2% Cur, supplementation for the present study, which was equivalent to about 1.2 g of Cur consumption daily for a 60 kg adult according to a published formula [16]. The diets were frozen in −20°C under vacuum package and fresh diets were provided to mice weekly. Before and after the treatment, the basal metabolic rate (oxygen consumption [VO_2], carbon dioxide production [VCO_2], respiratory exchange ratio [RER], and heat production] of mice during the day (quiescent phase) was measured using an Oxymax indirect open-circuit calorimetry system (Columbus Instruments, Columbus, OH, USA). After depriving the mice of food for 4 h, the continuous measurement for 3 h (with water provided) was conducted (one measurement every 30s) [17]. We used the lowest 10 consecutive measures as the estimate of basal metabolic rate.

Food intake and body weight were monitored weekly during the feeding trial. The metabolic efficiency was expressed as follows: metabolic efficiency = average weekly weight gain/average weekly food intake. At the end of week 10, mice were fasted overnight and sacrificed by carbon dioxide anesthesia followed by cervical dislocation. Blood samples were obtained into EDTA-containing tubes by cardiac puncture, and centrifuged at 4°C to collect plasma. The adipose tissues including the interscapular BAT, inguinal WAT (IngWAT) and epididymal WAT (EpiWAT), heart, kidney, and liver were rapidly isolated and weighed. The bulk of the adipose tissues were rapidly frozen in liquid nitrogen and then transferred to the −80°C freezer for further analysis, and the rest were fixed in 4% paraformaldehyde for sectioning and staining.

Table 2
Primer sequences used for real-time quantitative PCR

Gene	Forward (5′-3′)	Reverse (5′-3′)	Size (bp)	Access No.
18s	GTAACCCGTTGAACCCCATT	CCATCCAATCGGTAGTAGCG	151	NR_046233.2
FAS	TGAATCAGCCCCACGCAGT	CCGAGTCAGTCTTGGAGGACAT	297	NM_007988.3
SREBP-1c	GCAGCCACCATCTAGCCTG	CAGCAGTGAGTCTGCCTTGAT	199	NM_001358315.1
ACCα	TTCACTGTGGCTTCTCCAGC	GACCACCGACGGATAGATCG	125	XM_011248667.1
SCD1	ATTGAGTGCCGAGTCTGTGG	GCAAGGCACTTCTGAAACCG	191	XM_017321456.1
PPARα	TTGAAGGAGCTTTGGGAAGA	AGGAAGCCGTTCTGTGACAT	243	NM_001113418.1
CPT-1α	GACTCCGCTCGCTCATTCC	GACTGTGAACTGGAAGGCCA	96	NM_013495.2
PDK4	ACAGACATCATAATGTGGTCCCT	GGTCGATACTTCCAATGTGGC	213	NM_013743.2
MCAD	AGCTGATTGGCAATGTCTCCAGCAAA	GATCGCAATGGGTGCTTTTGATAGAA	291	NM_007382.5
Cox7a1	CAGCGTCATGGTCAGTCTGT	AGAAAACCGTGTGGCAGAGA	112	NM_009944.3
CD137	GTCGACCCTGGACGAACTGCTCT	CCTCTGGAGTCACAGAAATGGTGGTA	132	NM_001077590.1
Tbx1	TGAAGAAGAACCCGAAGGTGG	ACTTGGAACGTGGGGAACATT	133	XM_006536887.1
TMEM26	GAAACCAGTATTGCAGCACCCAAT	AATATTAGCAGGAGTGTTTGGTGGA	205	NM_177794.3
UCP1	ACTGCCACACCTCCAGTCATT	CTTTGCCTCACTCAGGATTGG	123	NM_009463.3
PGC-1α	CCCTGCCATTGTTAAGACC	TGCTGCTGTTCCTGTTTTC	161	XM_006503779.1
Elovl3	GATGGTTCTGGGCACCATCTT	CGTTGTTGTGTGGCATCCTT	73	XM_006526624.1
Cidea	ATCACAACTGGCCTGGTTACG	TACTACCCGGTGTCCATTTCT	136	NM_007702.2
PRDM16	CAGCACGGTGAAGCCATTC	GCGTGCATCCGCTTGTG	87	NM_001291029.1
IL-6	GAGGATACCACTCCCAACAGACC	AAGTGCATCATCGTTGTTCATACA	141	NM_001314054.1
TNFα	TGGGACAGTGACCTGGACTGT	TTCGGAAAGCCCATTTGAGT	67	NM_001278601.1
IL-1β	TCGCTCAGGGTCACAAGAAA	CATCAGAGGCAAGGAGGAAAC	73	XM_006498795.3
Glut4	CTCTCAGGCATCAATGCTGTTTTCTA	CGAGACCAACGTGAAGACCGTATT	123	NM_001359114.1

ACCα, acetyl-CoA carboxylase α; CD137, cluster of differentiation 137;; Cidea, cell death-inducing DFFA-like effector A; Cox7a1, cytochrome c oxidase subunit VIIa polypeptide 1; CPT-1α, carnitine palmitoyltransferase-1α; Elovl3, elongation of very long-chain fatty acids protein 3; FAS, fatty acid synthase; Glut 4, glucose transporter 4; IL, interleukin; MCAD, medium-chain acyl-CoA dehydrogenase; PCR, polymerase chain reaction; PDK4, pyruvate dehydrogenase kinase 4; PGC-1α, peroxisomal proliferator-activated receptor γ coactivator-1α; PPARα, peroxisome proliferator-activated receptor α; PRDM16, PR domain-containing 16; SREBP-1c, sterol regulatory element-binding protein-1c; Tbx1, T-box 1; TMEM26, transmembrane protein 26; TNF, tumor necrosis factor; UCP1, uncoupling protein 1

In vitro oxygen consumption assay

Isolated IngWAT (20 mg) was minced and cultured in a respiration buffer (2% bovine serum albumin, 1.1 mM sodium pyruvate, and 25 mM glucose in phosphate-buffered saline). Dissolved oxygen was measured before and after 25-min incubation using an Orion 3-Star Dissolved Oxygen Meter (Thermo Scientific, Waltham, MA, USA). The result was normalized to tissue weight [18].

Plasma irisin measurement

Plasma irisin concentration was determined by using a commercially available enzyme-linked immunosorbent assay (ELISA) kit (Arigobio, China) according to the manufacturer's instructions.

Histological analysis

Paraffin-embedded BAT and IngWAT sections (5-μm thick) were either stained with hematoxylin and eosin or used for UCP1 immunohistochemical (IHC) staining as previously described [19]. Imaging was performed using an EVOS microscope (Advanced Microscopy Group, Bothell, WA, USA). At least four images per section and four sections from each individual mouse were analyzed. Adipocyte size and number were measured by Image-Pro Plus 6.0 (Media Cybernetics, Rockville, MD, USA).

Quantitative real-time PCR analysis

Total RNA was extracted from different adipose tissue using Trizol reagent (Sigma-Aldrich, St. Louis, MO, USA) in accordance with the manufacturer's instructions, followed by reverse-transcription to cDNA using iScript™ cDNA Synthesis Kit (Bio-Rad, Hercules, CA, USA). Quantitative real-time polymerase chain reaction (qRT-PCR) was performed on the CFX96 RT-PCR Detection System (Bio-Rad) as described previously [20]. The relative mRNA expression of target genes was calculated and normalized with 18S ribosomal RNA reference using the method of $2^{-\Delta\Delta CT}$ [21]. The used primer sequences are shown in Table 2.

Immunoblotting analysis

Immunoblotting analyses was performed as previously described [22]. Briefly, protein extracts from adipose tissues were separated by 10% sodium dodecyl sulfate polyacrylamide gel electrophoresis and then transferred to polyvinylidene fluoride membrane. After blocking with 5% non-fat dry milk in Tris-buffered saline and Tween 20 (TBST), membranes were overnight incubated at 4°C with primary antibodies (1:1000), followed by incubation with horseradish peroxidase (HRP)-linked secondary antibody anti-rabbit immunoglobulin G or anti-mouse IgG in TBST for 1 h at room temperature. Finally, membranes were visualized using Bio-Rad ChemiDoc™ imaging system (Bio-Rad). Band density of target protein was quantified after normalization to β-actin content. Primary antibodies against UCP1, cytochrome C (Cyto C), nuclear factor κB (NF-κB) subunit p65, phosphorylated-NF-κB p65 (p-p65) at Ser536, c-jun N-terminal kinase (JNK), phosphorylated-JNK (p-JNK) at Thr183/Tyr185, protein kinase C-θ (PKCθ), phosphorylated-PKCθ (p-PKCθ) at Ser676, insulin receptor subunit (IRS)-1, phosphorylated-IRS-1 (p-IRS-1) at Ser307, protein kinase B (Akt), phosphorylated-Akt (p-Akt) at Ser473, p38 mitogen-activated protein kinase (p38 MAPK), phosphorylated-p38 MAPK (p-p38 MAPK) at Thr180/Tyr182, extracellular signal-related kinase (ERK) 1/2, phosphorylated-ERK1/2 (p-ERK1/2), β-actin and HRP-linked secondary antibody were purchased from Cell Signaling (Danver, MA, USA). FNDC5 polyclonal antibody was purchased from Abcam (Cambridge, MA, USA).

Table 3
The body weight measurements and organ index

	LFD	HFD	HFD + Cur
Body weight measurements			
Initial body weight, g	21.73 ± 0.29	21.71 ± 0.31	21.69 ± 0.33
Final body weight, g	27.87 ± 0.36^{c}	39.39 ± 1.18^{a}	35.37 ± 0.69^{b}
Average weekly food intake (g/wk)	23.14 ± 0.90^{a}	18.67 ± 0.37^{b}	18.75 ± 0.39^{b}
Average weekly weight gain (g/wk)	0.61 ± 0.04^{c}	1.79 ± 0.12^{a}	1.37 ± 0.06^{b}
Metabolic efficiency	0.026 ± 0.002^{c}	0.096 ± 0.008^{a}	0.073 ± 0.004^{b}
Relative organ weight (mg/g body weight)			
Inguinal fat pad	8.99 ± 0.32^{c}	24.95 ± 2.43^{a}	17.15 ± 2.75^{b}
Epididymal fat pad	12.27 ± 0.72^{c}	49.07 ± 3.36^{a}	33.04 ± 5.17^{b}
Brown fat pad	3.43 ± 0.26	4.01 ± 0.35	3.72 ± 0.29
Liver	44.80 ± 1.86	47.42 ± 2.21	43.65 ± 1.86
Heart	6.78 ± 0.40^{a}	4.59 ± 0.31^{b}	5.72 ± 0.60^{ab}
Kidney	13.48 ± 0.41^{a}	10.01 ± 0.63^{b}	11.19 ± 0.47^{b}

Cur, curcumin; HFD, high-fat diet; LFD, low-fat diet
Data expressed as mean ± SE. n = 10/group. Mean values with different letters are significantly different ($P < 0.05$)

Statistical analysis

All data sets were checked and confirmed to have normal distribution. Statistical analyses were performed by the one-way analysis of variance (ANOVA) followed by Tukey's test to compare the differences between treatments, using SPSS version 21 (IBM, Armonk, NY, USA). Results are presented as mean ± SEM. A significant difference was considered as $P<0.05$.

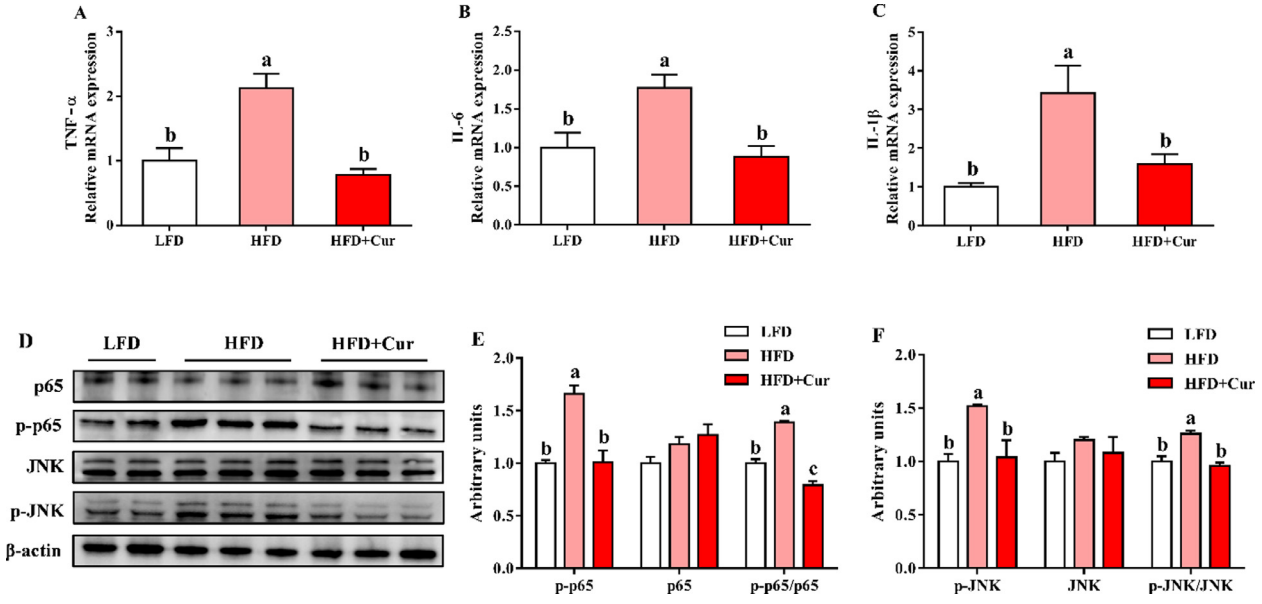

Fig. 1. Curcumin attenuates inflammatory responses in IngWAT of HFD-fed mice. (**A-C**) mRNA expression of TNF-α (**A**), IL-6 (**B**) and IL-1β (**C**). (**D**) representative images of immunoblotting. (**E**) relative protein contents of p65 and p-p65. (**F**) relative protein contents of JNK and p-JNK. Data were expressed as mean ± SE. n = 10/group. Mean values with different letters are significantly different ($P < 0.05$). Cur, curcumin; HFD, high-fat diet; IngWAT, inguinal white adipose tissue; LFD, low-fat diet; TNF, tumor necrosis factor.

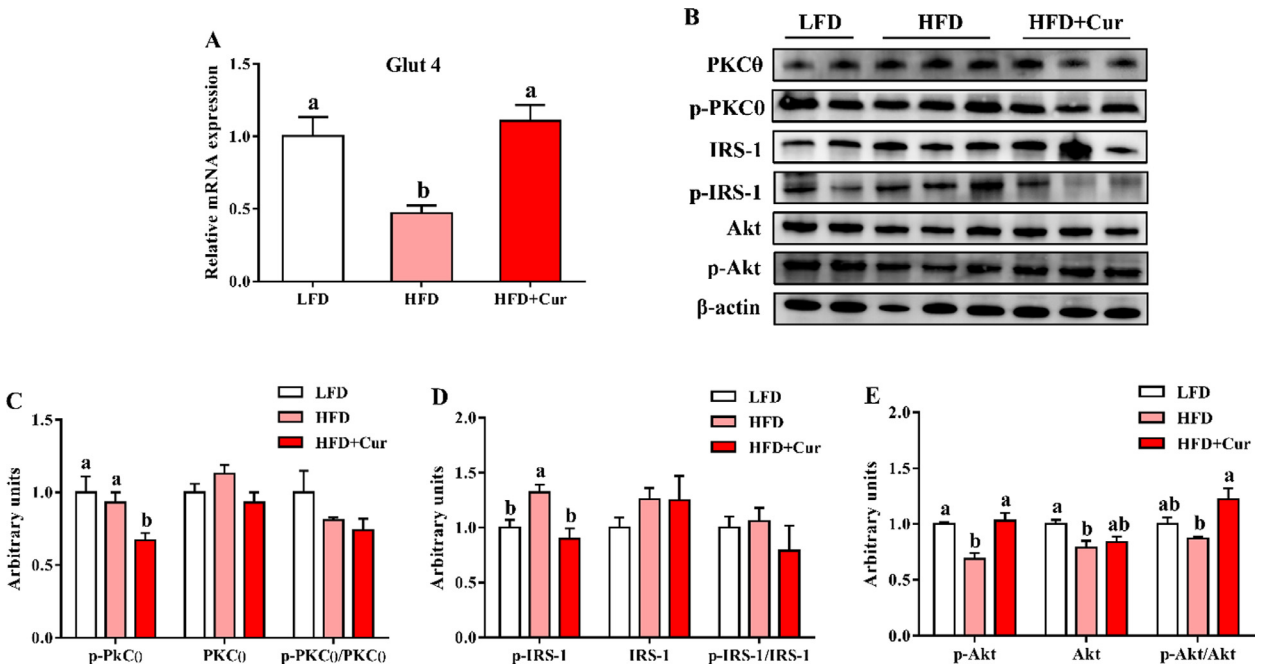

Fig. 2. Curcumin prevents insulin resistance in IngWAT of HFD-fed mice. (**A**) mRNA expression of *Glut4*. (**B**) representative images of immunoblotting. (**C**–**E**) relative protein contents of PKCθ and p-PKCθ (**C**), IRS-1 and p-IRS-1 (**D**), Akt and p-Akt (**E**). Data were expressed as mean ± SE. n = 10/group. Mean values with different letters are significantly different ($P < 0.05$). Cur, curcumin; HFD, high-fat diet; IngWAT, inguinal white adipose tissue; LFD, low-fat diet.

Results

Curcumin alleviates adiposity and inflammation in IngWAT of HFD-fed mice

HFD mice had higher body weight and the ratio of WAT mass to body weight than LFD mice. Dietary curcumin protected mice against HFD-induced body weight gain and fat accumulation. The average weekly food intake was similar between HFD and HFD + Cur mice. However, Cur-treated HFD mice had lower average weekly weight gain than HFD mice. Thus, the metabolic efficiency was decreased in HFD + Cur mice (Table 3).

Ectopic fat deposition in adipose tissues commonly contributes to chronic inflammation [23]. We found that the HFD feeding increased the mRNA expression of tumor necrosis factor (TNF)-α, interleukin (IL)-6, and IL-1β in IngWAT, which was prevented by Cur administration (Fig. 1A–C). Moreover, the NF-κB inflammatory pathway was enhanced in HFD mice as indicated by increased phosphorylation level of p65, which was again suppressed by dietary curcumin supplementation (Fig. 1D,E). A similar pattern of changes was observed for JNK, indicating the activation of JNK/MAPK pathway (Fig. 1D and F).

Curcumin prevents IR in IngWAT of HFD-fed mice

Inhibition of inflammation ameliorates IR [24]. As described previously in our lab, Cur-treated HFD mice had a better tolerance to glucose load and insulin sensitivity, which suggested that Cur administration improved whole body glucose homeostasis and insulin signaling [25]. Here, we found that the HFD feeding

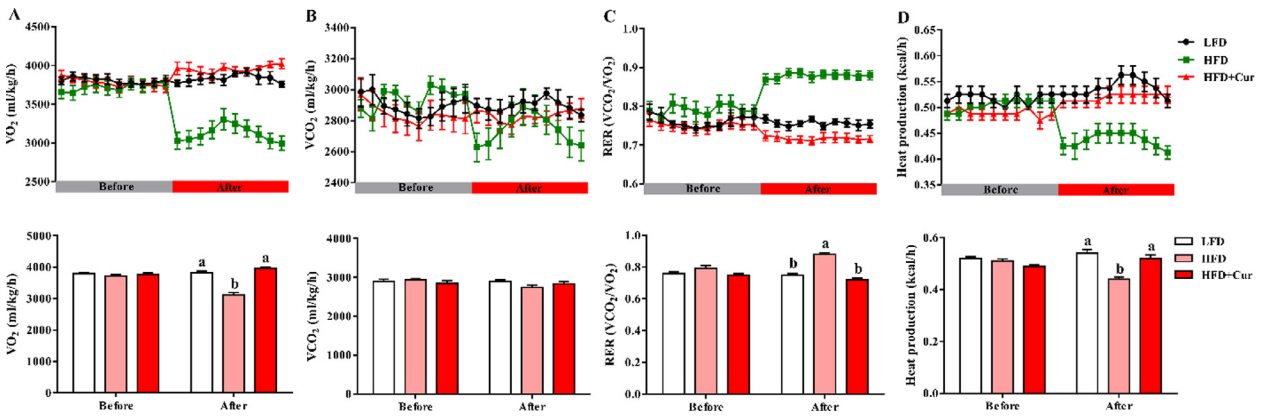

Fig. 3. Curcumin improves basal metabolic rate in HFD-fed mice. (**A**) Oxygen consumption during a 3-h period measured in a metabolic cage. (**B**) Carbon dioxide production during a 3-h period measured in a metabolic cage. (**C**) The RER value (VCO2/VO2) was calculated during a 3-h period. (**D**) Heat production during a 3-h period. Data were expressed as mean ± SE. n = 8/group. Mean values with different letters are significantly different ($P < 0.05$). Cur, curcumin; HFD, high-fat diet; LFD, low-fat diet; RER, respiratory exchange ratio; VCO_2, carbon dioxide production; VO_2, oxygen consumption.

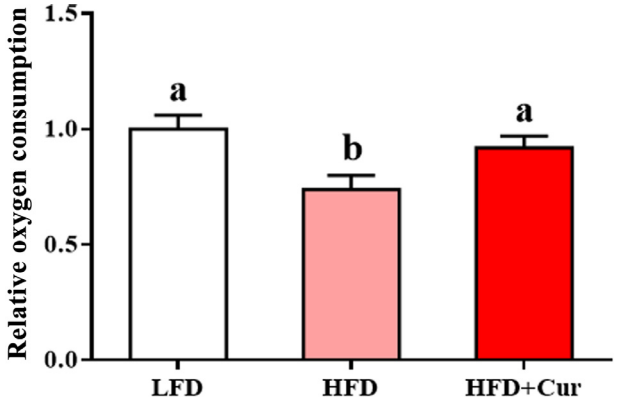

Figure 4. Curcumin increases the oxygen consumption of IngWAT in vitro. Data were expressed as mean ± SE. n = 8/group. Mean values with different letters are significantly different ($P < 0.05$). Cur, curcumin; HFD, high-fat diet; IngWAT, inguinal white adipose tissue; LFD, low-fat diet.

decreased glucose transporter 4 (Glut4) mRNA expression (Fig. 2A) and Akt (Ser473) phosphorylation (Fig. 2B and E), which were restored by Cur supplementation. Additionally, the phosphorylation of PKCθ at Ser676 and IRS-1 at Ser307 in IngWAT of HFD mice were reduced by Cur intake (Fig. 2B–D).

Curcumin improves metabolic rate in HFD-fed mice

To test whether Cur-treated mice exhibited metabolic alterations, the basal metabolic rate was determined before and after Cur administration. Cur treatment significantly increased the oxygen consumption compared with the HFD group, whereas Cur supplementation had no effect on carbon dioxide production (Fig. 3A, B). As a result, the RER (VCO_2/VO_2) of HFD + Cur mice was lower than that of the HFD mice after Cur administration, suggesting a higher ratio of lipid oxidation in HFD + Cur group (Fig. 3C). Furthermore, Cur supplementation increased heat production, showing higher basal energy expenditure (Fig. 3D). Consistently, Cur also increased basal oxygen consumption of IngWAT in vitro (Fig. 4).

Curcumin enhances BAT metabolic activity in HFD-fed mice

To explore the mechanisms improving energy expenditure in Cur-treated mice, BAT metabolic activity was further examined. Morphologically, BAT became filled with large lipid droplets in HFD mice, a phenotype similar to white fat, which was recovered by Cur administration (Fig. 5A). Moreover, Cur-treated mice showed greater UCP1 expression in BAT compared with HFD mice (Fig. 5A). In agreement, the UCP1 mRNA and protein levels were decreased in HFD mice but recovered by Cur supplementation (Fig. 5B–D). Correspondingly, Cur consumption also increased the mRNA expression of thermogenic genes, including PR domain-containing 16 (PRDM16), PGC-1α, elongation of very long-chain fatty acid protein 3 (Elovl3) and cytochrome C oxidase subunit VIIa polypeptide 1 (Cox7a1; Fig. 5B). Cur treatment of HFD mice increased Cyto C protein level (Fig. 5C,D), accompanied by upregulated expression of oxidative markers, including carnitine palmitoyltransferase-1α (CPT-1α), pyruvate dehydrogenase kinase 4 (PDK4) and peroxisome proliferator-activated receptor α (PPARα; Fig. 5E), indicating increased fatty acid oxidation upon Cur treatment. Together, these results suggested that curcumin increased metabolic activity in BAT of HFD mice.

Curcumin induces brown-like changes in IngWAT of HFD-fed mice

In response to nutritional stimuli, inguinal WAT can generate thermogenic beige/brown adipocytes [3]. Histologic analysis indicated that Cur-treated mice had smaller adipocytes and displayed more beige adipocytes and higher UCP1-positive areas in IngWAT

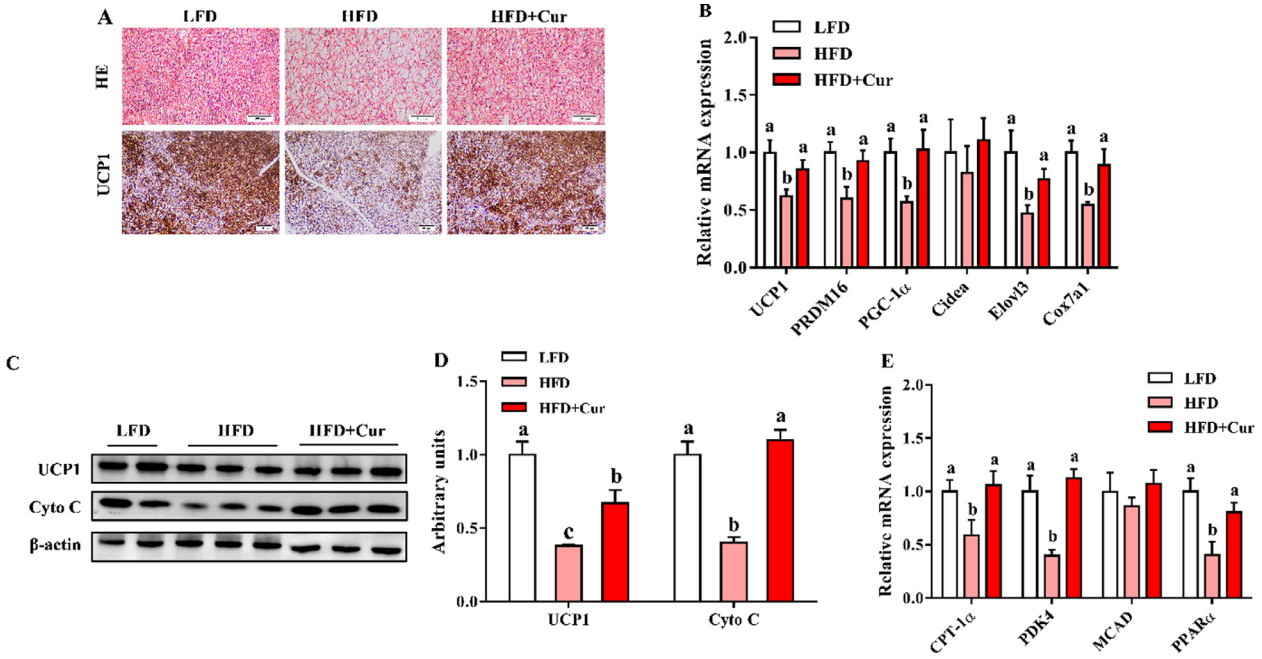

Fig. 5. Curcumin increases BAT metabolic activity in HFD-fed mice. (**A**) representative H&E staining and UCP1 staining for BAT sections (scale bar 100 μm). (**B**) mRNA expression of thermogenic genes in BAT. (**C**) representative images of immunoblotting. (**D**) relative protein contents of UCP1 and Cyto C. (**E**) mRNA expression of fatty acid oxidative markers. Data were expressed as mean ± SE. n = 10/group. Means values with different letters are significantly different ($P < 0.05$). BAT, brown adipose tissue; Cur, curcumin; Cyto C, cytochrome C; H&E, hematoxylin and eosin; HFD, high-fat diet; LFD, low-fat diet; UCP, uncoupled protein.

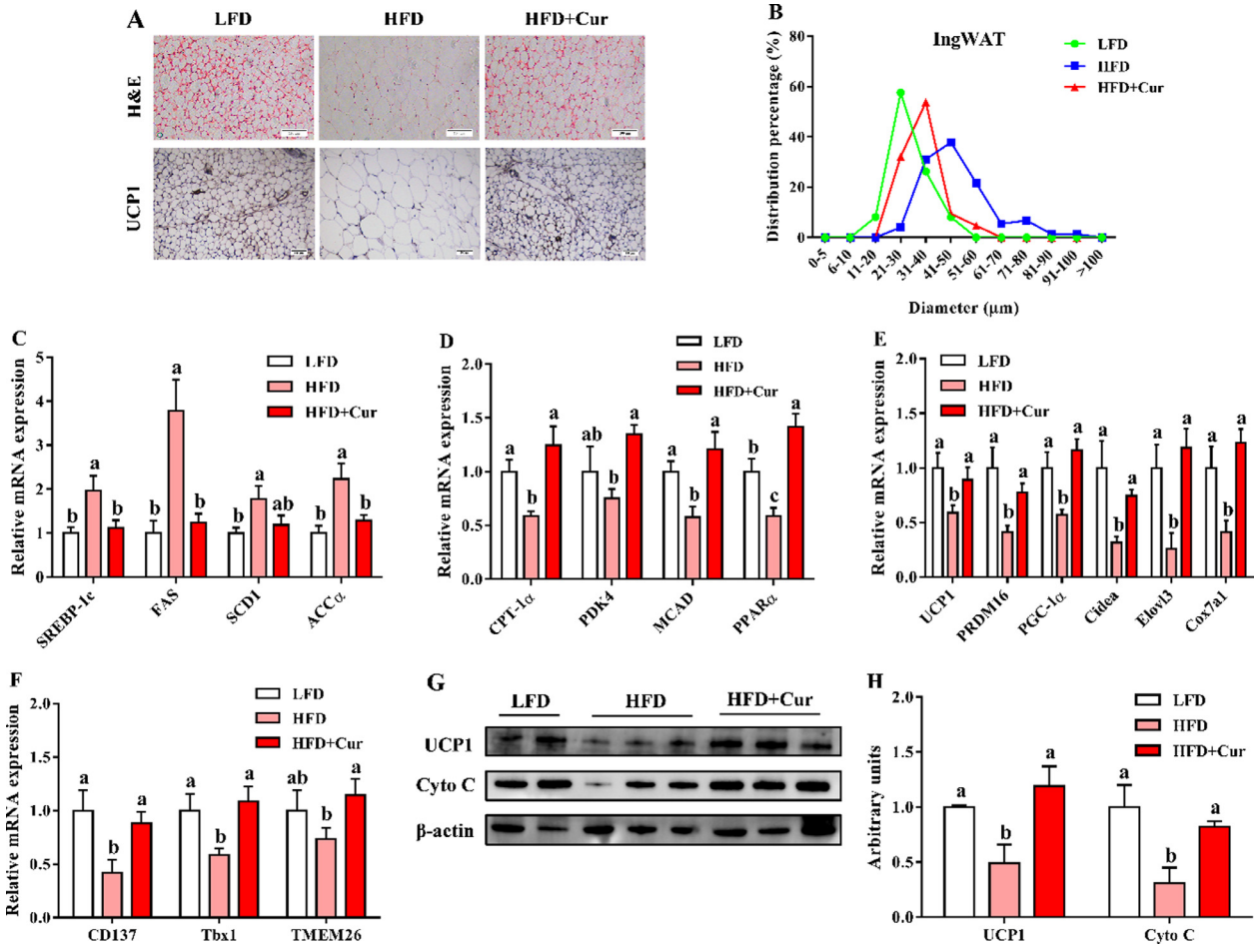

Fig. 6. Curcumin induces brown fat-like changes in IngWAT of HFD-fed mice. (**A**) representative H&E staining and UCP1 staining in IngWAT. (**B**) Percentage distribution of adipocyte diameters of IngWAT. (**C**) mRNA expression of lipogenesis genes. (**D**) mRNA expression of fatty acids oxidative markers. (**E**) mRNA expression of thermogenic genes. (**F**) mRNA expression of beige cell markers. (**G**) representative images of immunoblotting. (**H**) relative protein content of UCP1 and Cyto C. Data were expressed as mean ± SE. n = 10 per group. Means values with different letters are significantly different ($P < 0.05$). Cur, curcumin; Cyto C, cytochrome C; H&E, hematoxylin and eosin; HFD, high-fat diet; LFD, low-fat diet; UCP, uncoupled protein.

than those of HFD mice (Fig. 6A,B). Consistent with these findings, HFD remarkably enhanced the expression of lipogenesis genes, including sterol regulatory element-binding protein-1c (SREBP-1c), fatty acid synthase (FAS), and acetyl-CoA carboxylase α (ACCα), which were prevented by Cur administration (Fig. 6C). Among oxidative markers, dietary Cur supplementation increased the expression of CPT-1α, PDK4, medium-chain acyl-CoA dehydrogenase (MCAD), and PPARα (Fig. 6D). Moreover, UCP1 mRNA and protein expression were decreased in IngWAT of HFD, which was recovered by Cur intake (Fig. 6E, G, and H). Correspondingly, dietary curcumin supplementation increased the expression of a series of thermogenic genes in IngWAT of HFD mice, including PRDM16, PGC-1α, cell death-inducing DFFA-like effector A (Cidea), Elovl3, and Cox7a1 (Fig. 6E). A similar pattern of changes was observed for the mRNA expression of beige adipocyte-selective markers, including cluster of differentiation 137 (CD137), T-box 1 (Tbx1) and transmembrane protein 26 (TMEM26; Fig. 6F). Curcumin treatment of HFD mice increased Cyto C protein level, an important component of mitochondrial respiratory chain, in IngWAT (Fig. 6G,H). Token together, these results suggested that Cur supplementation drives the browning of IngWAT in HFD mice.

Curcumin activates FNDC5/irisin pathway in IngWAT of HFD-fed mice

FNDC5/irisin, a potential adipokine secreted by IngWAT, is known to stimulate browning of WAT [12]. Mice of HFD + Cur group had higher plasma irisin concentration compared with the HFD group, showing that Cur promoted the production and secretion of irisin (Fig. 7A). FNDC5 protein level was decreased in IngWAT of HFD mice but recovered by Cur administration (Fig. 7B and D). HFD feeding decreased the phosphorylation of p38 MAPK and ERK1/2, which was again restored by Cur supplementation, indicating that the possible involvement of p38 MAPK and ERK1/2 signaling in irisin-induced browning of white fat (Fig. 7B, C, and E).

Discussion

Obesity could partly be characterized by decreased metabolic efficiency of BAT and excessive WAT expansion and adipocyte hypertrophy [26]. Enhancement of thermogenic function in brown and beige adipocytes can improve obesity and related metabolic dysfunction via the ability of these cells to expend excess energy as heat. Cur is known for its beneficial effects in preventing obesity and ameliorating metabolic abnormalities [10,27,28], but only a

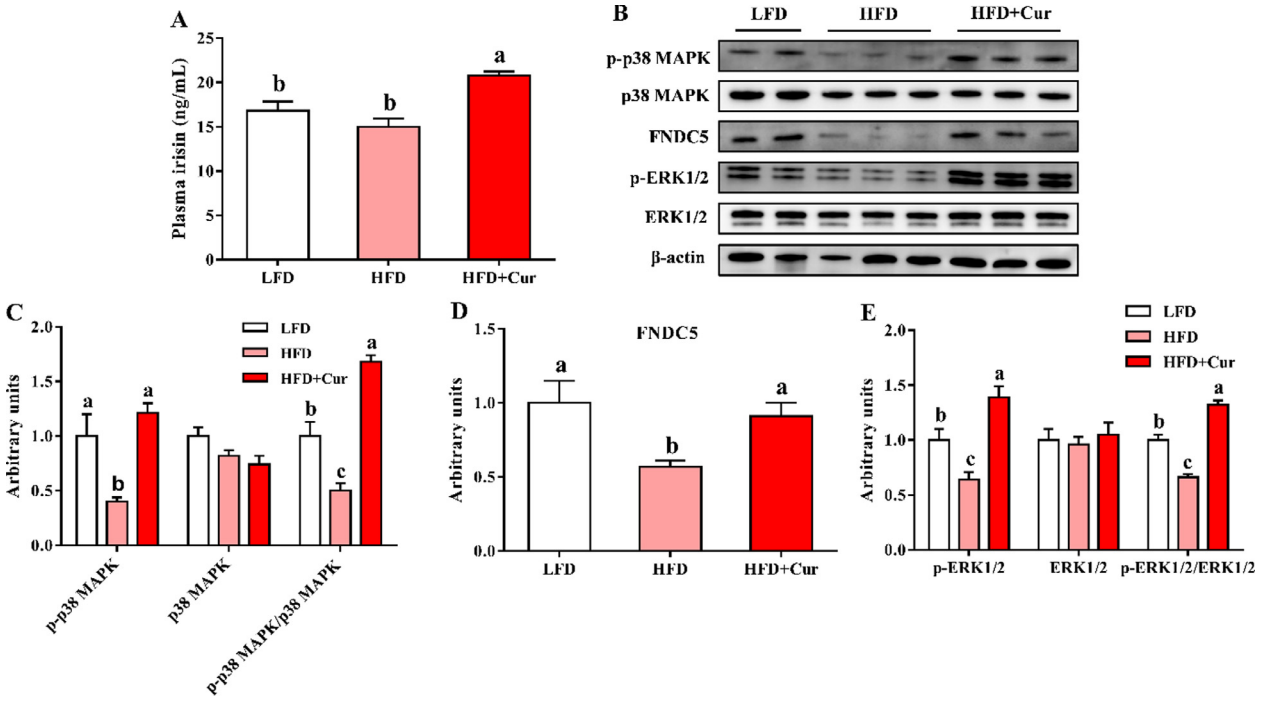

Fig. 7. Curcumin activates FNDC5/irisin pathway in IngWAT of HFD-fed mice. (**A**) plasma irisin concentration. (**B**) representative images of immunoblotting. (**C**–**E**) relative protein contents of p38 MAPK and p-p38 MAPK (**C**), FNDC5 (**D**), ERK1/2 and p-ERK1/2 (**E**). Data were expressed as mean ± SE. n = 10/group. Means values with different letters are significantly different ($P < 0.05$). Cur, curcumin; HFD, high-fat diet; LFD, low-fat diet.

few studies focus on energy metabolism and related molecular mechanism. The present study demonstrated that Cur alleviated adiposity by improving insulin sensitivity and remodeling whole body energy metabolism in associated with activation of FNDC5/p38MAPK/ERK pathways.

WAT of obese individuals are in a state of chronic inflammation characterized by increased proinflammatory cytokines expression such as TNF-α, IL-6, and IL-1β and activation of NF-κB and JNK signaling [29]. Protein p65 is a key mediator of inflammation cascades [30]. A recent study demonstrated that dietary Cur intervention promotes anti-inflammatory activity on white fat tissue in HFD-fed mice [5]. Consistently, Cur supplementation suppressed NF-κB and JNK signaling and decreased the expression of proinflammatory markers in IngWAT of obese mice, which might contribute to improved insulin sensitivity [31].

Tyrosine-phosphorylated IRS-1 protein, which is a key mediator of insulin signaling, stimulates the expression and translocation of Glut4 by activating the phosphatidylinositol 3-kinase (PI3K)/Akt pathway [32]. However, increasing IRS-1 serine phosphorylation impairs IRS-1-mediated insulin signaling by antagonizing its tyrosine phosphorylation, contributing to IR [33,34]. Moreover, the activation of PKCθ increases IRS-1 serine phosphorylation, which enhanced HFD-induced defects in insulin signaling and glucose transport in WAT [35,36]. In the present study, we found that Cur supplementation reduced PKCθ phosphorylation at Ser676, associated with decreased phosphorylation of IRS-1 (Ser307) and activation of Akt as well as *Glut4* gene expression, indicating an improved insulin sensitivity in IngWAT. Similarly, recent study demonstrated that dietary Cur enhances insulin clearance by restoring PI3K and Akt levels in obese mice [4].

As determined by an indirect calorimetry, Cur administration enhanced whole body energy expenditure, as evidenced by oxygen consumption and heat production assay, which contributes to the improved metabolic rate and suppression of obesity-related pathologic factors. In accordance, our in vitro data further indicated that Cur increased the basal oxygen consumption of IngWAT in obese mice. The increased energy expenditure induced by Cur are related partly to the enhanced BAT and WAT metabolic function. WAT stores excess excessive energy via adipocyte hypertrophy and hyperplasia. Differently, brown and beige adipocytes promote energy expenditure via non-shivering thermogenesis, attenuating obesity and IR [2,37]. BAT burns fatty acids and glucose to produce heat, which is capable of generating 300 times more heat than other tissues per unit mass [38]. PRDM16 is a key transcription factor driving brown adipogenesis and thermogenesis, which induces the genes expression of UCP1 and PGC-1α [39]. Our present results indicated Cur enhanced the expression of PRDM16 and UCP1 and other thermogenic genes in BAT of HFD mice, indicating an improved thermogenesis. Additionally, Cyto C, an essential electron transport chain component highly enriched in BAT, plays a crucial role in regulating mitochondrial oxidative phosphorylation [40]. As expected, we found that Cur increased Cyto C protein level in BAT of HFD mice, which may imply the stimulatory action of Cur on fatty acid oxidation. Meanwhile, Cur supplementation upregulated the expression of oxidative markers in BAT of HFD mice. This is consistent with the decreased RER in Cur-treated mice. These results advanced our knowledge on the beneficial effects of Cur on BAT metabolic function.

To our knowledge, there is limiting evidence on the underlying mechanism of Cur in promoting WAT browning. The development and thermogenesis of beige adipocytes in WAT are regulated by a complex network of hormones and signaling pathways, of which the FNDC5/irisin pathway is important [41,42]. PGC-1α overexpression induces FNDC5 expression and irisin secretion, which acts on WAT to stimulate brown-like adipocyte formation by increasing UCP1 expression [11]. More importantly, irisin-induced improvements in glucose metabolism and browning of fat is probably mediated by p38 MAPK and ERK1/2 signaling pathways [41,43]. In

this study, we found that Cur treatment increased circulating plasma irisin levels and FNDC5 expression and the phosphorylation of p38 MAPK and ERK1/2 in IngWAT of HFD mice, along with improvements in whole-body glucose homeostasis and insulin sensitivity as evidenced by our previous study [25]. These results indicated that FNDC5-irisin/p38 MAPK/ERK1/2 may mediate the well-known beneficial effects of Cur on insulin sensitivity and beige adipocyte formation, optimizing energy metabolism in obese individuals.

Conclusion

The present results demonstrated that dietary Cur supplementation alleviated HFD-induced adipocyte hypertrophy and inflammation by improving insulin sensitivity and energy metabolism and enhancing thermogenic program both in BAT and WAT, which was associated with activation of FNDC5/p38MAPK/ERK pathways. This study suggests that dietary Cur may be a good candidate as a safe and potential agent in preventing adiposity and also provides a functional mechanism for the observed Cur-induced improvements in energy metabolism.

References

[1] Almoosawi S, Vingeliene S, Karagounis LG, Pot GK. Chrono-nutrition: a review of current evidence from observational studies on global trends in time-of-day of energy intake and its association with obesity. Proc Nutr Soc 2016;75:487–500.
[2] Bartelt A, Heeren J. Adipose tissue browning and metabolic health. Nature Rev Endocrinol 2014;10:24–36.
[3] Silvester AJ, Aseer KR, Yun JW. Dietary polyphenols and their roles in fat browning. J Nutr Biochem 2019;64:1–12.
[4] Kim Y, Rouse M, Gonzalez-Mariscal I, Egan JM, O'Connell JF. Dietary curcumin enhances insulin clearance in diet-induced obese mice via regulation of hepatic PI3K-AKT axis and IDE, and preservation of islet integrity. Nutr Metab (Lond) 2019;16:48.
[5] Song Z, Revelo X, Shao W, Tian L, Zeng K, Lei H, et al. Dietary curcumin intervention targets mouse white adipose tissue inflammation and brown adipose tissue UCP1 expression. Obesity 2018;26:547–58.
[6] Adiwidjaja J, McLachlan AJ, Boddy AV. Curcumin as a clinically-promising anticancer agent: pharmacokinetics and drug interactions. Expert Opin Drug Metab Toxicol 2017;13:953–72.
[7] Jurenka JS. Anti-inflammatory properties of curcumin, a major constituent of Curcuma longa: a review of preclinical and clinical research. Altern Med Rev 2009;14:141–53.
[8] Feng D, Zou J, Su D, Mai H, Zhang S, Li P, et al. Curcumin prevents high-fat diet-induced hepatic steatosis in ApoE(-/-) mice by improving intestinal barrier function and reducing endotoxin and liver TLR4/NF-kappaB inflammation. Nutr Metab (Lond) 2019;16:79.
[9] Cheng AL, Hsu CH, Lin JK, Hsu MM, Ho YF, Shen TS, et al. Phase I clinical trial of curcumin, a chemopreventive agent, in patients with high-risk or pre-malignant lesions. Anticancer Res 2001;21:2895–900.
[10] Lone J, Choi JH, Kim SW, Yun JW. Curcumin induces brown fat-like phenotype in 3T3-L1 and primary white adipocytes. J Nutr Biochem 2016;27:193–202.
[11] Boström P, Wu J, Jedrychowski MP, Korde A, Ye L, Lo JC, et al. A PGC1-α-dependent myokine that drives brown-fat-like development of white fat and thermogenesis. Nature 2013;481:463–8.
[12] Arturo RR, Cecilia C, Senin LL, Landrove MO, Javier B, Belén CA, et al. FNDC5/irisin is not only a myokine but also an adipokine. PLoS One 2013;8:e60563.
[13] Niranjan SB, Belwalkar SV, Tambe S, Venkataraman K, Mookhtiar KA. Recombinant irisin induces weight loss in high fat DIO mice through increase in energy consumption and thermogenesis. Biochem Biophys Res Commun 2019;519:422–9.
[14] Mahgoub MO, D'Souza C, Al Darmaki R, Baniyas M, Adeghate E. An update on the role of irisin in the regulation of endocrine and metabolic functions. Peptides 2018;104:15–23.
[15] Takano K, Tatebe J, Washizawa N, Morita T. Curcumin inhibits age-related vascular changes in aged mice fed a high-fat diet. Nutrients 2018:10.
[16] Shannon RS, Minakshi N, Nihal A. Dose translation from animal to human studies revisited. Faseb J 2008;22:659–61.
[17] Wang S, Liang X, Yang Q, Fu X, Rogers C, Zhu M, et al. Resveratrol induces brown-like adipocyte formation in white fat through activation of AMP-activated protein kinase (AMPK) α1. Int J Obesity 2015;39:967–76.
[18] Yang Q, Liang X, Sun X, Zhang L, Fu X, Rogers CJ, et al. AMPK/α-ketoglutarate axis dynamically mediates DNA demethylation in the Prdm16 promoter and brown adipogenesis. Cell Metab 2016;24:542–54.
[19] Zou T, Wang B, Li S, Liu Y, You J. Dietary apple polyphenols promote fat browning in high-fat diet-induced obese mice through activation of adenosine monophosphate-activated protein kinase alpha. J Sci Food Agric 2020;100:2389–98.
[20] Zou T, Wang B, Yang Q, Avila JMD, Zhu MJ, You J, et al. Raspberry promotes brown and beige adipocyte development in mice fed high-fat diet through activation of AMP-activated protein kinase (AMPK) α1. J Nutr Biochem 2018;55:157–64.
[21] Livak KJ, Schmittgen TD. Analysis of relative gene expression data using real-time quantitative PCR and the $2^{-\Delta\Delta CT}$ method. Methods 2001;25:402–8.
[22] Zou T, Chen D, Yang Q, Wang B, Zhu MJ, Nathanielsz PW, et al. Resveratrol supplementation to high fat diet-fed pregnant mice promotes brown and beige adipocyte development and prevents obesity in male offspring. J Physiol 2017;595:1547–62.
[23] Rasouli N, Molavi B, Elbein S, Kern P. Ectopic fat accumulation and metabolic syndrome. Diabetes Obes Metab 2010;9:1–10.
[24] Olefsky JM, Glass CK. Macrophages, inflammation, and insulin resistance. Annu Rev Physiol 2010;72:219–46.
[25] Li S, You J, Wang Z, Liu Y, Wang B, Du M, et al. Curcumin alleviates high-fat diet-induced hepatic steatosis and obesity in association with modulation of gut microbiota in mice. Food Res Int 2021;143:110270.
[26] Bluher M. Obesity: global epidemiology and pathogenesis. Nat Rev Endocrinol 2019;15:288–98.
[27] Nishikawa S, Kamiya M, Aoyama H, Nomura M, Hyodo T, Ozeki A, et al. Highly dispersible and bioavailable curcumin but not native curcumin induces brown-like adipocyte formation in mice. Mol Nutr Food Res 2018;62.
[28] Wang S, Wang X, Ye Z, Xu C, Zhang M, Ruan B, et al. Curcumin promotes browning of white adipose tissue in a norepinephrine-dependent way. Biochem Bioph Res Co 2015;466:247–53.
[29] Longo M, Zatterale F, Naderi J, Parrillo L, Miele C. Adipose tissue dysfunction as determinant of obesity-associated metabolic complications. Int J Mol Sci 2019;20:2358.
[30] Ye J, Keller JN. Regulation of energy metabolism by inflammation: A feedback response in obesity and calorie restriction. Aging 2010;2:361–8.
[31] Shoelson SE, Herrero L, Naaz A. Obesity, inflammation, and insulin resistance. Gastroenterology 2014;132:2169–80.
[32] Copps KD, White MF. Regulation of insulin sensitivity by serine/threonine phosphorylation of insulin receptor substrate proteins IRS1 and IRS2. Diabetologia 2012;55:2565–82.
[33] Tian S, Jia W, Lu M, Zhao J, Sun X. Dual-specificity tyrosine phosphorylation-regulated kinase 1A ameliorates insulin resistance in neurons by up-regulating IRS-1 expression. J Biol Chem 2019;294:20164–76.
[34] Zou T, Kang Y, Wang B, de Avila JM, You J, Zhu MJ, et al. Raspberry supplementation reduces lipid accumulation and improves insulin sensitivity in skeletal muscle of mice fed a high-fat diet. J Funct Foods 2019;63:103572.
[35] Zhou J, Wang Q, Ding Y, Zou MH. Hypochlorous acid via peroxynitrite activates protein kinase Ctheta and insulin resistance in adipocytes. J Mol Endocrinol 2015;54:25–37.
[36] Li Y, Soos TX, Wu J, Degennaro M, Sun X, Littman DR, et al. Protein kinase C Theta inhibits insulin signaling by phosphorylating IRS1 at Ser(1101). J Biol Chem 2004;279:45304–7.
[37] Okla M, Kim J, Koehler K, Chung S. Dietary factors promoting brown and beige fat development and thermogenesis. Adv Nutr 2017;8:473–83.
[38] Symonds ME. Brown adipose tissue growth and development. Scientifica 2013;2013:305763.
[39] Seale P, Conroe HM, Estall J, Kajimura S, Frontini A, Ishibashi J, et al. Prdm16 determines the thermogenic program of subcutaneous white adipose tissue in mice. J Clin Invest 2011;121:96–105.
[40] Lu R, Ji H, Chang Z, Su S, Yang G. Mitochondrial development and the influence of its dysfunction during rat adipocyte differentiation. Mol Bio Rep 2010;37:2173–82.
[41] Zhang Y, Xie C, Wang H, Foss RM, Clare M, George EV, et al. Irisin exerts dual effects on browning and adipogenesis of human white adipocytes. Am J Physiol Endocrinol Metab 2016;311:E530–41.
[42] Li H, Zhang Y, Wang F, Donelan W, Zona MC, Li S, et al. Effects of irisin on the differentiation and browning of human visceral white adipocytes. Am J Transl Res 2019;11:7410–21.
[43] Zhang Y, Li R, Meng Y, Li S, Donelan W, Zhao Y, et al. Irisin stimulates browning of white adipocytes through mitogen-activated protein kinase p38 MAP kinase and ERK MAP kinase signaling. Diabetes 2014;63:514–25.